

Article

Release Behavior of High Molecular Weight Solutes from Poly(ethylene glycol)-Based Degradable Networks

Sanxiu Lu, and Kristi S. Anseth

Macromolecules, **2000**, 33 (7), 2509-2515 • DOI: 10.1021/ma9915024 • Publication Date (Web): 15 March 2000

Downloaded from <http://pubs.acs.org> on April 13, 2009

More About This Article

Additional resources and features associated with this article are available within the HTML version:

- Supporting Information
- Links to the 9 articles that cite this article, as of the time of this article download
- Access to high resolution figures
- Links to articles and content related to this article
- Copyright permission to reproduce figures and/or text from this article

[View the Full Text HTML](#)



Release Behavior of High Molecular Weight Solutes from Poly(ethylene glycol)-Based Degradable Networks

Sanxiu Lu and Kristi S. Anseth*

Department of Chemical Engineering, University of Colorado, Boulder, Colorado 80309-0424

Received September 1, 1999; Revised Manuscript Received February 7, 2000

ABSTRACT: Water-soluble PEG-based macromers containing oligomeric blocks of a hydrolyzable α -hydroxy acid were synthesized and photopolymerized to form degradable hydrogels to control the release of high molecular weight, hydrophilic solutes. First, network mesh size and volume swelling ratio during the degradation process were characterized to understand fundamentally the effect of hydrogel degradation kinetics and subsequent changes in network structure on solute release. Second, the release behavior was examined and related to the swelling and structural properties of the hydrogels; experimental results show that solute transport can be diffusion controlled or degradation controlled depending on the relative size of the hydrogel mesh size to the solute. Finally, the ability to tailor the release from multilaminated biodegradable hydrogels to obtain an approximate zero-order release profile was studied theoretically.

Introduction

Hydrogels are hydrophilic polymers that are cross-linked to form insoluble, but water-swallowable, networks. Hydrogels have been used as drug carriers for controlled drug delivery for several decades.^{1,2} The applications of hydrogels are strongly linked to their excellent biocompatibility, flexibility in tailoring physiochemical properties, such as permeability and swelling, and the ability to load drugs without the loss of their bioactivity.²

Nondegradable hydrogels have been extensively studied for diffusion-controlled and swelling-controlled delivery devices.^{3–5} In the design of drug delivery devices used as implants, however, it is highly desirable to utilize biodegradable hydrogels. Degradation avoids removal of the device from the body by surgery or other means when the device is no longer needed. Additionally, because delivery can be controlled primarily through the degradation of the polymer, biodegradable hydrogels also provide flexibility in the design of delivery systems for large molecular weight drugs, such as peptides and proteins, which are not suitable for diffusion-controlled release through nondegradable hydrogel matrices. Therefore, biodegradable hydrogels have been developed in recent years to prepare new and better drug delivery systems by combining the unique properties of hydrogels with various degradation mechanisms.

The materials of interest in this research were hydrolytically degradable hydrogels formed from poly(ethylene glycol) α -hydroxy acid block copolymers end-capped with photocurable acrylate groups first developed by Hubbell and co-workers.⁶ Hubbell et al. used these hydrogels to release high molecular weight pharmaceutical;^{7,8} however, few studies have been performed to correlate underlying hydrogel degradation kinetics, and subsequent changes in network structure, with drug release. The study of solute transport in hydrogels necessitates a through characterization of the polymer diffusional space available for transport. Therefore, to gain a fundamental understanding of drug release from biodegradable hydrogels, the first objective of this research was to characterize the degradable hydrogels

during the degradation process and investigate quantitatively and experimentally the influence of degradation of the hydrogel matrix on the release kinetics of high molecular weight solutes. In particular, we wanted to understand how the macromer composition affects the polymer degradation properties, relate the degradation-dependent network swelling to an average mesh size of the network, and determine how the mesh size variations correlate to the solute release behavior.

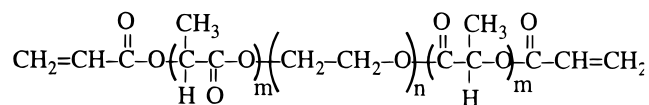
Since the physical structure of the polymeric material affects solute release rates through the solute diffusion coefficient, investigation of solute transport through cross-linked hydrogels requires quantitative analysis of solute diffusion coefficients in the macromolecular mesh of the polymer. To understand and better interpret the release results from these biodegradable hydrogels, the experimentally obtained time-dependent hydrogel properties were related to time-dependent solute diffusivity to predict the release behavior from monolithic release matrices studied here.

In addition to simulating solute release from uniform hydrogel matrix devices, the modeling work was further extended to multilaminated matrix devices. Multilamination techniques allow for the fabrication of nonhomogeneous matrix devices where parameters such as the degradation chemistry and solute loading can be varied in each laminate to control the release behavior. Previously, we developed a photolaminating technique to prepare multilaminated matrix devices, in which the polymer material and drug concentration in each constitute layer can be easily controlled.^{5,9–11} In addition, we developed a simulation technique to model drug release from multilaminated nondegradable hydrogel matrices with constant solute diffusivity and any initial concentration profiles. For the macromers studied here, degradable multilaminated matrices can be synthesized wherein time-dependent as well as spatial-dependent properties can be varied throughout the matrix to control the release behavior. When these biodegradable hydrogels are laminated heterogeneously together, the resulting nonuniform initial solute diffusivity in the assembly and a time-dependent solute diffusivity in each constitute layer can be manipulated to influence significantly the overall solute release behavior. In this

* To whom correspondence should be addressed.

Table 1. Release Solutes with Selected Relevant Properties

solute	MW (Da)	Stokes' radius (Å)	solubility in water at 25 °C (mg/mL)	diffusivity at 37 °C in aq soln (10 ⁻⁵ mm ² /s)
lysozyme	14 100	16.0	10.0	2.17
bovine serum albumin (BSA)	65 000	34.8	40.0	1.00
FITC-dextrin (dextrin)	77 000	55.0	>25.0	0.63

**Figure 1.** Chemical structure of macromer copoly(PEG-*b*-D,L-lactic acid) diacrylates.

study, the simulation technique was extended to examine the effects of nonconstant solute diffusivity on solute release from degradable multilaminated matrix devices.

Experimental Section

Materials. Poly(ethylene glycol)s (PEGs) with molecular weights 3400, 4600, and 8000 Da were obtained from Aldrich, and D,L-lactide (LA) was obtained from Polysciences. Other chemicals used in the macromer synthesis were stannous octoate (Sigma), triethylamine (Aldrich), acryloyl chloride (Aldrich), dichloromethane (Sigma), and anhydrous diethyl ether (Aldrich). All were of reagent grade and used as received. The photoinitiator 2,2-dimethoxy-2-phenylacetophenone (DMPA, Aldrich) was dissolved in *N*-vinylpyrrolidone (NVP, Aldrich) to form a 600 mg/mL solution of DMPA prior to use. NVP was chosen due to its amphiphilicity and biocompatibility⁸ and because it helps reduce the extractable sol fraction. Three hydrophilic, macromolecular solutes were studied, as listed in Table 1 along with the solute molecular weight, Stokes' radius, and solubility in water at 25 °C.¹² An estimation of the solute diffusivity in dilute aqueous solution at 37 °C was calculated using the Stokes–Einstein equation¹³ (eq 1), and the results are listed in Table 1.

$$r_s = \frac{k_B T}{6\pi\eta D_0} \quad (1)$$

In this equation, r_s is the Stokes–Einstein hydrodynamic radius of the solute, k_B is Boltzmann's constant, T is temperature, η is the viscosity of water at T , and D_0 is the solute diffusivity in water at T .

Methods. For the preparation of the macromer, we adopted the method of Hubbell.⁶ Briefly, the macromer was synthesized in a two-step process. In the first step, the dihydroxy poly(ethylene glycol) was reacted with D,L-lactide for 6 h at 160–200 °C using stannous octoate as a catalyst under vacuum and argon atmosphere. Then, the intermediate block copolymer was dissolved in methylene chloride, precipitated in anhydrous diethyl ether, and vacuum filtered followed by desiccating for a minimum of 24 h before use. In the second step, the intermediate block copolymer was acrylated. The intermediate block copolymer was dissolved in methylene chloride, and a 3-fold excess of triethylamine was added to the solution followed by adding dropwise a 3-fold excess of acryloyl chloride. The mixture was then reacted at 0 °C for 12 h followed by at room temperature for 12 h under vacuum and argon atmosphere to add an acrylate unit to each end of the macromer. The final macromer structure is shown in Figure 1, where m is the number of lactoyl units per end and n is the number of ethylene glycol units. The distribution of the lactoyl units in the lactide copolymers was confirmed by NMR experimental results.⁶ Specifically, 3400 Da PEG with 0, 3, and 5 lactoyl units per end (3.4KL0, 3.4KL3, and 3.4KL5) and 4600 Da PEG and 8000 Da PEG with 5 lactoyl units per end (4.6KL5, 8KL5) were synthesized.

For hydrogel synthesis, a 20–40 wt % macromer solution was made by dissolving macromers at the desired concentration in HEPES-buffered saline (pH 7.4, 10 mM), and 2 μ L of

the photoinitiator solution was added to each 1 g of the macromer solution. For the release experiments, various solutes (0.4–1.0 wt %) were then added to the macromer solutions. The resulting solutions were pipetted into a mold between two glass microscope slides and exposed to 365 nm UV light (Blak-Ray, nominal intensity 10 mW/cm²) for several minutes until the polymerization was complete. The resulting polymer hydrogels were cropped to the desired disk shape (1–2 mm in thickness, 13.8 mm in diameter) and characterized experimentally as described below.

In characterizing the degradation behavior of hydrogels for controlled release applications, the volume swelling ratio (Q) is an important parameter. Volume swelling ratio is the volume of the swollen matrix per unit volume of dry polymer matrix. This parameter is a function of the hydrophilicity of the network as well as the degree of cross-linking and the network structure. Knowledge of the equilibrium degree of swelling allows for calculation of matrix structural parameters such as the molecular weight between cross-links and the mesh size of the gel. Experimentally, one gel was placed in a vial containing 10 mL of the HEPES buffer, which was placed in a water bath at 37 °C. At a predetermined time, the gel was removed and weighed in air, $W_{a,deg}$, and in heptane, $W_{h,deg}$. Then, the gel was dried under vacuum and room temperature until constant weight followed by weighing in air, $W_{a,dry}$, and in heptane, $W_{h,dry}$. The Q was calculated according to eq 2.

$$Q = \frac{(W_{a,deg} - W_{h,deg})/\rho_h}{(W_{a,dry} - W_{h,dry})\rho_h} \quad (2)$$

Here the density of heptane, ρ_h , is 0.684 g/cm³.

For the hydrogel networks prepared from the photopolymerizable copoly(PEG-*b*-D,L-lactic acid) diacrylates, the macromers are cross-linked through their acrylate end groups. The average molecular weight between cross-links, \bar{M}_c , and hence the mesh size of the network, was determined from equilibrium swelling measurements. The average molecular weight between cross-links, \bar{M}_c , was calculated using the Flory–Rehner equation.¹⁴

$$\frac{1}{\bar{M}_c} = \frac{2}{\bar{M}_n} - \frac{\bar{v}_1(\ln(1 - v_2) + v_2 + \chi_1 v_2^2)}{v_2^{1/3} - \frac{v_2}{2}} \quad (3)$$

where \bar{M}_n is the number-average molecular weight of the uncross-linked polymer (the molecular weight of the macromer), V_1 is the molar volume of the solvent (18 cm³/mol), v_2 is the polymer volume fraction in the equilibrium swollen gel, which equals the reciprocal of the volume swelling ratio, Q , \bar{v} is the specific volume of the polymer, and χ is the polymer–solvent interaction parameter.

Since χ has not been experimentally determined for these novel hydrogels, we made two assumptions to estimate conservatively this value. As the molecular weight of the PLA was sufficiently small compared to that of the PEG segment in the macromers studied in this paper, the properties of the macromers in solution and the gel properties were assumed to be determined primarily by the PEG segment. A value for the PEG–solvent interaction parameter of 0.426¹⁵ was used in this investigation. In addition, since χ was found to be nearly independent of PEG polymer volume fraction in the ranges from 0.04 to 0.2,¹⁵ in which our experimental polymer volume fractions belong to, the value of the PEG–solvent interaction parameter was kept constant in calculating the mesh size.

Some limitations to these assumptions are discussed as followed. First, the existence of PLA makes the macromer more hydrophobic than PEG, which may result in a higher value of χ than 0.426 for the macromer. In addition, χ may vary with degradation time as the hydrophilicity of the network changes.

The mesh size of the hydrogel network was determined as described by Canal and Peppas.¹⁶ The root-mean-squared end-to-end distance of the polymer chain in the unperturbed state was calculated using eq 4:

$$(\bar{r}_0^2)^{1/2} = lC_n^{1/2}n^{1/2} \quad (4)$$

where l is the bond length, C_n is the characteristic ratio of the polymer, and n is the number of bonds in the cross-link. The mesh size in angstroms, ξ , of the swollen polymer network was then calculated from

$$\xi = v_2^{-1/3}(\bar{r}_0^2)^{1/2} \quad (5)$$

For solute release experiments, the hydrogel was formed by photopolymerizing an aqueous solution of a macromer precursor, in which 0.4–1.0 wt % of a bioactive solute was dissolved to ensure homogeneous distribution throughout the hydrogel matrix after photopolymerization. Since photopolymerizations proceed very rapidly at room temperature, the entrapped solutes kept their stability during the UV irradiation. After photopolymerization, the disk-shaped gel was placed in a vial containing 10 mL of the HEPES buffer (pH = 7.4, 37 °C). At predetermined time points, samples of 2.4 mL were taken and replaced by fresh buffer. The protein concentrations of lysozyme and BSA were measured with the Bio-Rad protein assay using the microassay procedure,¹⁷ in which a differential color change of a dye occurs in response to various concentrations of protein. The concentration of FITC-dextran was monitored using a UV-vis spectrophotometer (Hewlett-Packard 8452A diode array) at 494 nm (the wavelength of maximum absorbance for FITC-dextran). Since the polymer degradation products interfere with the measurement of the solute concentration, the solutions from identical hydrogels without solute were used as a blank in analyzing the solute concentration as a function of degradation.

Results and Discussion

In biodegradable hydrogels, if the solute release is to be controlled by the degradation of the polymer, the characteristic dimensions, mobility, and degradation rate of the hydrogel must be matched to the size of the diffusing solute molecules. If the initial mesh size of the hydrogel is much larger than that of the solute to be released, the entrapped solute simply diffuses out of network with little influence of degradation. In addition, control of variations with mesh size in time is very important if one wants to design time-programmed solute delivery devices. Oftentimes, the water content increases with degradation, which further influences the release of entrapped molecules. Therefore, the parameters affecting the network mesh size and volume swelling ratio during the degradation process were investigated in this study.

The physical characteristics and the degradation behavior of the investigated hydrogels are controlled by three main factors: the type of α -hydroxy acid segment, the length of the α -hydroxy acid segment, and the molecular weight of the central PEG segment. For these highly swollen hydrogels, the degradation product lactic acid rapidly releases from the network, and hence, the effect of the degradation product on gel degradation was assumed to be negligible. We chose D,L-lactide as the degradable linkage in this study since its degradation rate allows timely collection of data based on our preliminary results;¹⁰ however, one may easily incor-

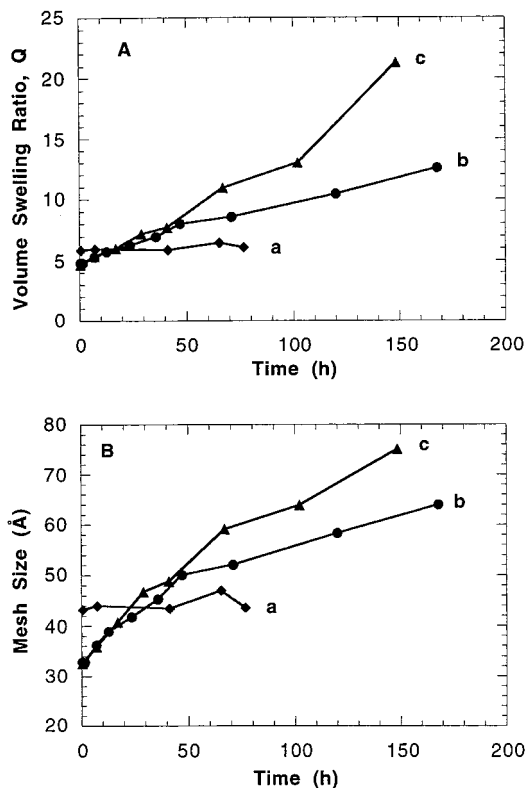


Figure 2. Effect of the length of lactide block on (A) volume swelling ratio and (B) network mesh size of the hydrogel network as a function of degradation time. The hydrogels were produced from macromers (a) 3.4KL0, (b) 3.4KL3, and (c) 3.4KL5.

porate ϵ -caprolactone or glycolide or copolymers to adjust further the degradation rate.

To examine the influence of the length of lactoyl repeat units on the variation of gel mesh size and volume swelling ratio with degradation time, hydrogels with fixed PEG molecular weight (3400 Da) and varied number of lactoyl repeat units (0, 3, 5) were prepared. The experimental results are presented in Figure 2. As shown in Figure 2A, the initial mesh size of the 3.4KL0 hydrogel network was slightly larger than that of 3.4KL3 and 3.4KL5 hydrogel networks, which was attributed to the lower gel fraction of 3.4KL0 (0.781) compared with those of 3.4KL3 (0.872) and 3.4KL5 (0.892).¹⁰ The initial mesh size of the 3.4KL3 and 3.4KL5 gel networks was almost the same value. Upon degradation, however, the variation in mesh size was significantly influenced by the length of lactoyl repeat units. In curve a, the 3.4KL0 macromer had no hydrolyzable lactoyl unit attached, and the mesh size of the polymer did not change over the time period examined. In curves b and c, the mesh size increased with degradation time as the ester linkages in the lactoyl repeat units were hydrolyzed. As the number of repeat lactoyl units increased from 3 to 5, the average variation of mesh size with degradation time increased from 4.5 to 6.9 Å/day over the time period examined.

The increased degradation rate was attributed to the longer hydrolyzable ester linkage. Upon exposure to water, the hydrogel undergoes random chain scission by simple hydrolysis of the ester linkage, in which every ester in the chain has an equal probability of being attacked. Therefore, the occurrence of chain scission of the macromer is proportional to the number of its hydrolyzable units; the longer the lactoyl repeat units,

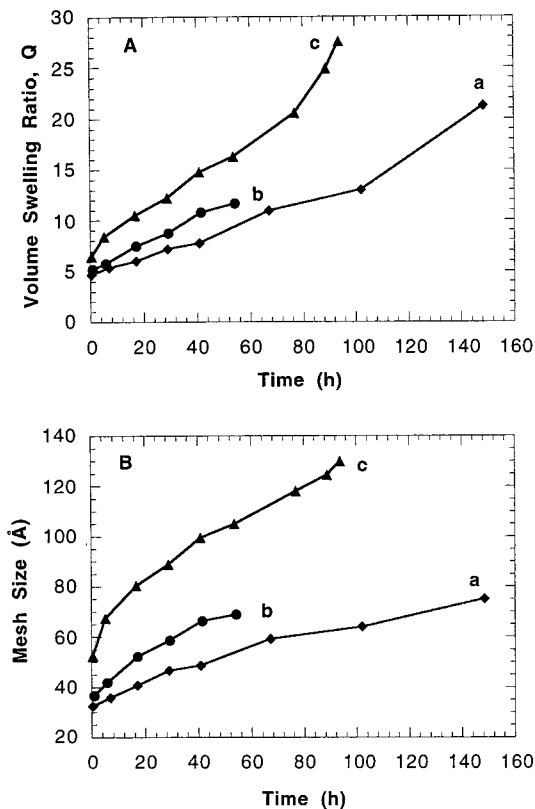


Figure 3. Effect of the length of PEG segment on (A) volume swelling ratio and (B) network mesh size of the hydrogel network as a function of degradation time. The hydrogels were produced from macromers (a) 3.4KL5, (b) 4.6KL5, and (c) 8KL5.

the higher probability of chain scission of the macromer and, hence, the higher the degradation rate. Further, when chain scission occurs on either end of the two extensions of the macromer, the cross-link breaks. The resulting network accommodates more water as demonstrated by the experimental results for the hydrogel volume swelling ratio (Figure 2B), and the increased water content in the hydrogel further promotes its hydrolysis rate. In addition, as experimentally observed, the time to reach complete degradation of the network decreased as the number of lactoyl repeat unit in the macromers increased. For example, the total degradation times for 3.4KL3, 3.4KL5, and 3.4KL10 hydrogels were 17, 10, and 4 days, respectively. It is worthy to mention that characterization of these gels with degradation is challenging as hydrolysis leads to increased swelling and the samples become extremely fragile and difficult to handle. We were able to follow the degradation quantitatively to about 50% mass loss.

In addition, experiments were conducted to investigate the effect of the molecular weight of the PEG segment on the gel mesh size and volume swelling ratio with degradation time. Figure 3 presents the results for hydrogels produced from 3.4KL5, 4.6KL5, and 8KL5 macromers. As illustrated in Figure 3A, when the PEG molecular weight changed from 3400 to 4600 to 8000 Da, the initial volume swelling ratio increased correspondingly as a result of the PEG hydrophilicity. Figure 3B also shows that the higher the PEG molecular weight, the larger the initial network mesh size, since a higher PEG molecular weight, and hence a higher macromer molecular weight, results in a lower cross-linking density of the hydrogel. Upon degradation, both

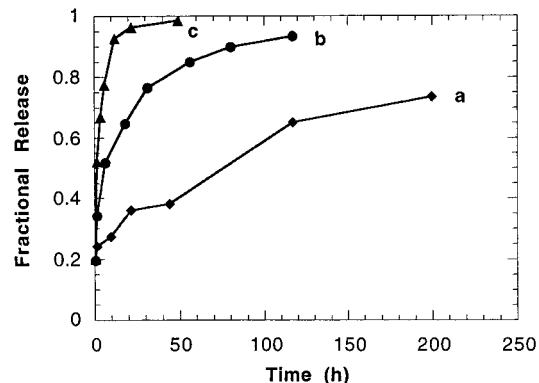


Figure 4. Cumulative release of lysozyme from hydrogels with different length of lactide segment as a function of release time. The hydrogels were produced from macromers (a) 3.4KL0, (b) 3.4KL3, and (c) 3.4KL5.

the network mesh size and the volume swelling ratio increase as discussed previously. In addition, the slopes of the curves for the volume swelling ratio and mesh size increase from curve a (3.4KL5) to curve b (4.6KL5) to curve c (8KL5).

The experimental results of Figures 2 and 3 show that the network mesh size and the volume swelling ratio increase with degradation time, and the variation of the two parameters with degradation time depends on the number of lactoyl repeat and PEG segment. To demonstrate that hydrogel mesh size and volume swelling ratio greatly affect the release behavior of encapsulated solutes, hydrogels with different number of lactoyl repeat unit (0, 3, 5) were used to release lysozyme, a model hydrophilic drug with a molecular weight of 14 100 Da and hydrodynamic radius of ~ 16.0 Å.

As shown in the experimental results (Figure 4), the lysozyme release profiles begin with a major release spike. Since the size of lysozyme (16.0 Å) is smaller than the initial mesh size of the three hydrogels (from 32 to 42 Å), lysozyme diffuses from the hydrogel unhindered, and the high solute concentration gradient at the beginning contributes to the burst effect. After this initial period, the release profiles exhibited significantly different release behavior depending on the composition of the hydrogel carriers. On average, computed from the slope of the release profiles from the initial burst effect to about 76% release, the lysozyme release rate was $\sim 0.0027\%/h$ for 3.4KL0, $0.018\%/h$ for 3.4KL3, and $0.104\%/h$ for 3.4KL5.

The difference in the release rates is closely related to the influence of the network degradation and subsequent network structure on the solute diffusivity. As will be discussed later, the solute diffusivity in hydrogels is closely related to the hydrogel mesh size and its volume swelling ratio (eq 6); the larger the hydrogel mesh size and volume swelling ratio, the larger the solute diffusion coefficient in hydrogel. Therefore, the solute diffusivity in the 3.4KL0 hydrogel does not change over time, and the solute release rate decreases with time as the solute concentration gradient decreases. In contrast, both the 3.4KL3 and 3.4KL5 gels exhibited an increased mesh size and volume swelling ratio with degradation time (Figure 2), leading to a higher solute diffusivity with degradation. The increased solute diffusivity counters the decreasing concentration gradient, and thus the overall solute release rate increases greatly from the nondegradable 3.4KL0 gel to the degradable 3.4KL3 gel and 3.4KL5 gel.

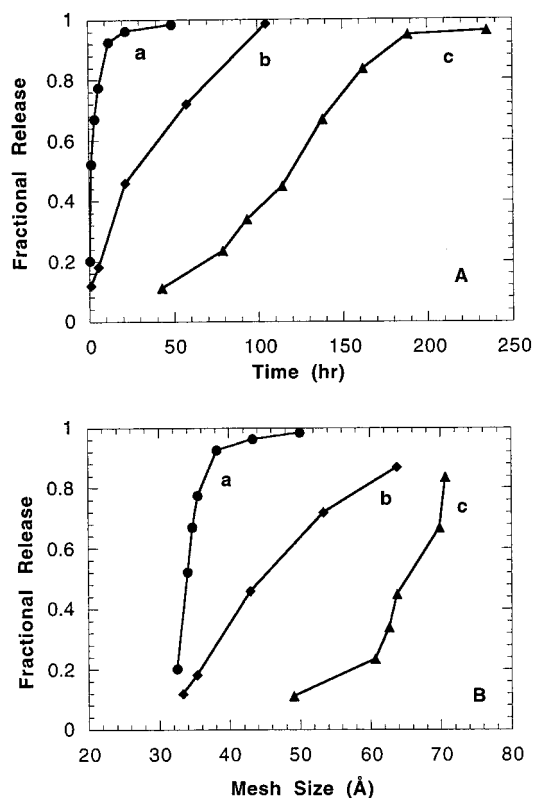


Figure 5. Effect of the molecular weight of the solutes on cumulative fractional release (A) as a function of release time and (B) as a function of hydrogel mesh size. The release solutes were (a) lysozyme, (b) BSA, and (c) dextran. The hydrogels were produced from the 3.4KL5 macromer.

To evaluate the dependence of the release rate on the size of the entrapped solute, a series of solutes with different molecular weights were incorporated into 3.4KL5 hydrogel disks. The chosen solutes were lysozyme, BSA, and FITC-dextran. As shown in Table 1, the molecular weight for these solutes ranges from 14 100 to 77 000 Da, and the hydrodynamic radius varies from 16.0 to 55.0 Å. The release profiles of these solutes were followed during the degradation of the gel. The experimental results of cumulative fractional release as a function of release time are shown in Figure 5A. In addition, the relationship between the solute release and the network mesh size was examined to gain further insight into understanding the effect of network mesh size on solute release, and the results are demonstrated in Figure 5B.

Experimental results shown in Figure 5A,B illustrate that there is a distinct correlation between the size of the solute, the network mesh size, and the overall release behavior. Although all of the solutes were able to diffuse from the 3.4KL5 hydrogel upon degradation, the release profiles were dramatically different depending on the solute size. As the solute size increased from 16 Å (curve a) to 34.8 Å (curve b) to 55 Å (curve c), the solute release rate decreased, and the solute release behavior was more closely coupled to the degradation process. For example, lysozyme was almost totally released at the beginning when the mesh size of the 3.4KL5 hydrogel was around its initial value (32 Å) because the lysozyme could readily diffuse from the network due to its small size (16 Å). However, there was negligible dextran (55 Å) release at the beginning because dextran size was much larger than the initial hydrogel mesh size. Upon degradation, as the mesh size

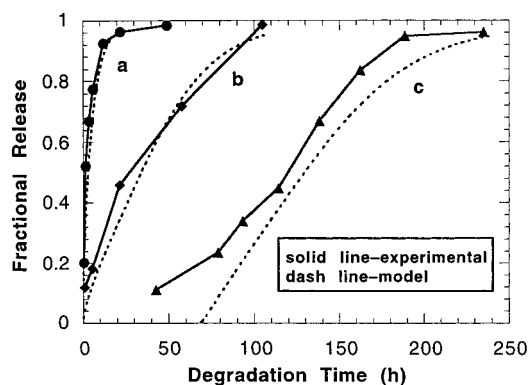


Figure 6. Simulating the effect of molecular weight of the solute (a) lysozyme, (b) BSA, and (c) dextran on cumulative fractional release. The solid lines were experimental data, and the dash lines were model data. The hydrogels were produced from the 3.4KL5 macromer.

of the network continuously increased and approached the solute size, the dextran began to release slowly. When the mesh size of the hydrogel was larger than the dextran size (~60 Å), the solute release rate greatly increased as indicated by a steeper release curve in Figure 5B.

As shown in the above experimental results, the mesh size and volume swelling ratio of the investigated degradable hydrogels increased with degradation time, and the variation of the two parameters was closely related to the solute release behavior. To describe quantitatively the influence of hydrogel degradation on solute release, free volume theory¹⁶ was used here to relate the change of the network structure with degradation time to a change in the time-dependent solute diffusivity affecting the solute release. For homogeneous hydrogels, there are many equations to describe the relationship between diffusivity and polymer structure based on free volume theory and hydrodynamic theory.^{2,18,19} Equation 6 was chosen to simulate our experimental data as the parameters are easily defined for our system.

$$\frac{D_g}{D_0} = \left(1 - \frac{r_s}{\xi}\right) \exp\left(-Y\left(\frac{\phi}{1-\phi}\right)\right) \quad (6)$$

In this equation, D_g is the solute diffusion in a gel, D_0 is the solute diffusion in the liquid at infinite dilution, r_s is the radius of the solute, ξ is the mesh size between cross-links, and ϕ is the volume fraction of polymer in the gel. Y is the ratio of the critical volume required for a successful translational movement of the solute molecule and the average free volume per molecule of the liquid. For correlation purposes, a good approximation for Y is unity.¹⁹

In our model, we used the experimentally determined network mesh size and the volume fraction of polymer in the gels to calculate the time-dependent solute diffusivity during the degradation process. Then the time-dependent diffusivity was used to simulate the solute release process using the well-known diffusional release for films with uniform initial drug loading.²⁰ Specifically, we simulated the release of lysozyme, BSA, and dextran from the 3.4KL5 hydrogel, and the modeling results are shown in Figure 6.

Figure 6 illustrates that the simulation data and experimental results agree quite well, especially for spheroidal molecules such as lysozyme and BSA. This

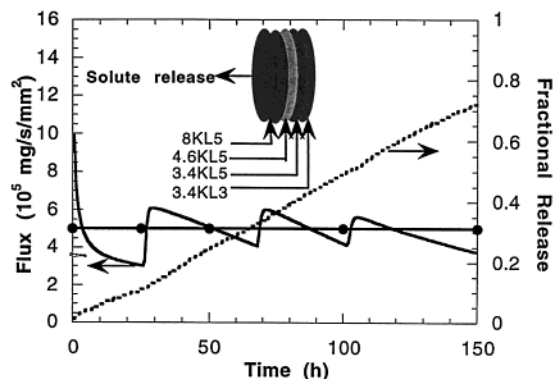


Figure 7. Simulation results of dextran release from a four-layer hydrogel matrix device with a uniform initial dextran concentration. The hydrogel materials were produced from macromers, from center outside, 3.4KL3, 3.4KL5, 4.6KL5, and 8KL5, respectively.

agreement indicates a time-dependent diffusivity can be used to account for both the Fickian-type diffusion of solute from the gel matrix and the release of solute upon the degradation of the gel. For the higher molecular weight solute dextran, however, there was a slightly greater deviation but fairly quantitative assuming the simplifications employed. First, the mesh size is an average spacing between cross-links in the polymer, and hence, some spaces between cross-links in the hydrogel are larger or smaller than the estimated mesh size. Dextran may release slowly from the hydrogel initially due to the heterogeneous distribution of cross-links as observed experimentally. Second, the Stokes–Einstein equation (eq 1) assumes that the solute has a spherical shape to calculate its hydrodynamic radius. The fact that dextran molecules have rodlike configurations indicates that the actual cross-sectional area of the molecule is smaller than the estimated one, and hence, the molecule has a better chance to be released from the polymer compared with the ideal spherical shape. This difference between the ideal and actual shape of dextran may explain the faster release rate in experimental profiles compared with the predicted data based on a spherical solute molecule.

As demonstrated above experimentally and theoretically, solute release behavior from single-layer biodegradable hydrogels greatly depends on the hydrogel properties; the same solute may display different release patterns in different hydrogel matrices. Furthermore, a multilaminated matrix with a different type of hydrogel or drug in each layer could provide unique advantages in controlling the actual release profile. To confirm this idea, solute release was modeled from a four-layer matrix device, where each layer contains a different matrix chemistry. For this simulation, dextran was used as a model solute, and a constant release rate (5×10^{-5} mg/(s mm²)) was desired. The solute concentration was uniformly distributed, and the hydrogel materials, from center outside, were produced from macromer 3.4KL3, 3.4KL5, 4.6KL5, and 8KL5, respectively. Mesh sizes and volume swelling ratios of these hydrogels during degradation process were previously characterized as presented in Figures 2 and 3.

In Figure 7, the solute release from the four-layer matrix device approaches zero order until 70% of the initially loaded drug was released. In this simulation, the initial burst effect is due to the larger initial mesh size of 8KL5 hydrogel compared to the solute size. The

burst effect can be easily controlled by choosing hydrogels that have smaller initial mesh sizes than the solute size. Since the initial mesh size of the 4.6KL5, 3.4KL5, and 3.4KL3 layers were smaller than the solute size, the solute release from these three constitute layers displayed induction periods as demonstrated by the three abruptly increased matrix flux in the release profile. This result is similar to the release of dextran in Figure 5A where the dextran release showed a delayed release due to the smaller initial network mesh size compared to the solute size. Experimentally, a smoother flux profile from the four-layer matrix would be expected due to the mobility of polymer chains and the existence of a distribution of hydrogel mesh size as discussed previously.

In addition to constant release behavior, more complex release pattern can be achieved from bulk degradation-controlled multilaminates by synthesizing and characterizing suitable biodegradable hydrogels and manipulating the initial network mesh size and the hydrogel degradation rate in each constitute layer. For example, a delayed-release system with a controlled time lag can be obtained by employing hydrogels with an initial mesh size smaller than the solute size. Moreover, the magnitude of the release rate can be easily manipulated by adjusting the solute concentration, and different types of solute can be loaded in each layer and released in a programmed method by manipulating the hydrogel property.

Conclusions

Degradable hydrogels, photopolymerized from water-soluble PEG-based macromers containing hydrolyzable oligomeric blocks of a hydrolyzable α -hydroxy acid, were used to control the release of high molecular weight hydrophilic solutes. The variation of the network mesh size and volume swelling ratio with degradation time was found to depend on the type and length of oligo(α -hydroxy acid), as well as the molecular weight of PEG sequence. Experimental release results show that the solute release behavior from these hydrogels is strongly affected by the relative value of the network mesh size and the hydrodynamic radius of the solute. When the hydrodynamic radius of the solute is much larger than the mesh size of the network, the solute release behavior is degradation-controlled. The experimental characterization of the network with degradation time was used to simulate the drug release behavior, and the resulting model data and experimental results agree quite well. Finally, model results demonstrate that approximate zero-order release behavior can be achieved from bulk degradation-controlled multilaminated matrix devices theoretically.

Acknowledgment. The authors thank the Packard Foundation for support of the work through a grant. The authors also acknowledge significant technical assistance from Kira Marciniak and Matthew Lipscomb.

References and Notes

- (1) Wichterle, O.; Lim, D. *Nature* **1960**, *185*, 117–119.
- (2) Peppas, N. A., Ed. *Hydrogels in Medicine and Pharmacy*; CRC Press: Boca Raton, FL, 1986; Vols. I–III.
- (3) Mathur, A. M.; Hammonds, K. F.; Klier, J.; Scranton, A. B. *J. Controlled Release* **1998**, *54*, 177–184.
- (4) Wroblewski, C.; Kopeckova, P.; Rihova, B. *Macromol. Chem. Phys.* **1998**, *199*, 2601–2608.

- (5) Lu, S.; Anseth, K. S. *J. Controlled Release* **1999**, *57*, 291–300.
- (6) Sawhney, J. S.; Pathak, C. P.; Hubbell, J. A. *Macromolecules* **1993**, *26*, 581–587.
- (7) Cruise, G. M.; Scharp, D. S.; Hubbell, J. A. *Biomaterials* **1998**, *19*, 1287–1294.
- (8) West, J. L.; Hubbell, J. A. *React. Polym.* **1995**, *25*, 139–147.
- (9) Lu, S.; Ramirez, F. R.; Anseth, K. S. *J. Pharm. Sci.*, in press.
- (10) Lu, S. Ph.D. Dissertation, Department of Chemical Engineering, University of Colorado, Boulder, 1999.
- (11) Lu, S.; Ramirez, F. W.; Anseth, K. S. *AIChE J.* **1998**, *44*, 1689–1696.
- (12) Amsden, B. *Macromolecules* **1998**, *31*, 8382–8395.
- (13) Bird, R. B.; Stewart, W. E.; Lightfoot, E. N. *Transport Phenomena*; John Wiley and Sons: Toronto, 1960.
- (14) Flory, P. J. *Principles of Polymer Chemistry*; Cornell University Press: Ithaca, NY, 1953.
- (15) Merrill, E. W.; Dennison, K. A.; Sung, C. *Biomaterials* **1993**, *14*, 1117–1126.
- (16) Canal, T.; Peppas, N. A. *J. Biomed. Mater. Res.* **1989**, *23*, 1183–1193.
- (17) Bradford, M. M. *Anal. Biochem.* **1976**, *72*, 248–254.
- (18) Cukier, R. I. *Macromolecules* **1984**, *17*, 252–255.
- (19) Lustig, S. R.; Peppas, N. A. *J. Appl. Polym. Sci.* **1988**, *36*, 735–747.
- (20) Crank, J. *The Mathematics of Diffusion*; Clarendon Press: Oxford, 1975.
MA9915024